10 Mechanisms of Flow and Sediment Transport in Fluvial Ecosystems: Physical and Ecological Consequences

Brett Eaton and Jordan Rosenfeld

10.1 Introduction

Anyone who has spent time in or around rivers will recognize that water flows in complex, ever-changing patterns that are in part determined by the physical shape and roughness of the stream boundaries. Low gradient, deep rivers may look almost like lakes, having very smooth water surfaces giving little indication that the water is flowing at all, while a great deal less water flowing through a steep, cobble-bedded mountain channel may form a turbulent, noisy maelstrom of whitewater (Figure 10.1). It is also true that these complex flow patterns imprint themselves physically upon the riverine environment by eroding, transporting and depositing sediment and organic material, thereby shaping the streams in which the water flows.

Channels that have developed within large deposits of sediment (i.e., floodplains, fans and deltas) have **alluvial channel boundaries**, meaning that they consist of the sediment transported and deposited by the river itself. These systems are particularly dynamic, in that the boundaries of the stream channel evolve at rates that are appreciable on human timescales; the evolution of these boundaries is determined by the interplay between the forces and energy associated with the flux of water in the stream channel and the quantity and texture of sediment delivered to a stream channel from the surrounding drainage basin. In this way, the behavior of stream at a given point can be influenced by processes happening anywhere in the drainage basin upstream. As the boundaries of these alluvial streams change, the aquatic ecosystems that they support must adapt.

Hutchinson (1965) described the environment as a stage where plant and animal species play out the theater of life. In many ecosystems, such as boreal and tropical forests on land, or kelp forests in the ocean, plants form much of the three-dimensional structure that forms the ecological stage where individual growth, survival, predation, competition, and community dynamics occur. In streams and rivers, it is the physical structure of the channel itself that forms the dominant habitat template that constrains ecological processes and the adaptations of aquatic organisms. All aspects of the ecology of aquatic organisms – from behavior, growth, and reproduction to avoiding predation – are mediated by the attributes of the flowing water environment. Consequently, ecologists can only hope to understand species adaptations, population dynamics, and ecosystem processes within the context of the physical structure and dynamic fluxes of stream habitats. Throughout this chapter we review the key hydraulic processes that shape the

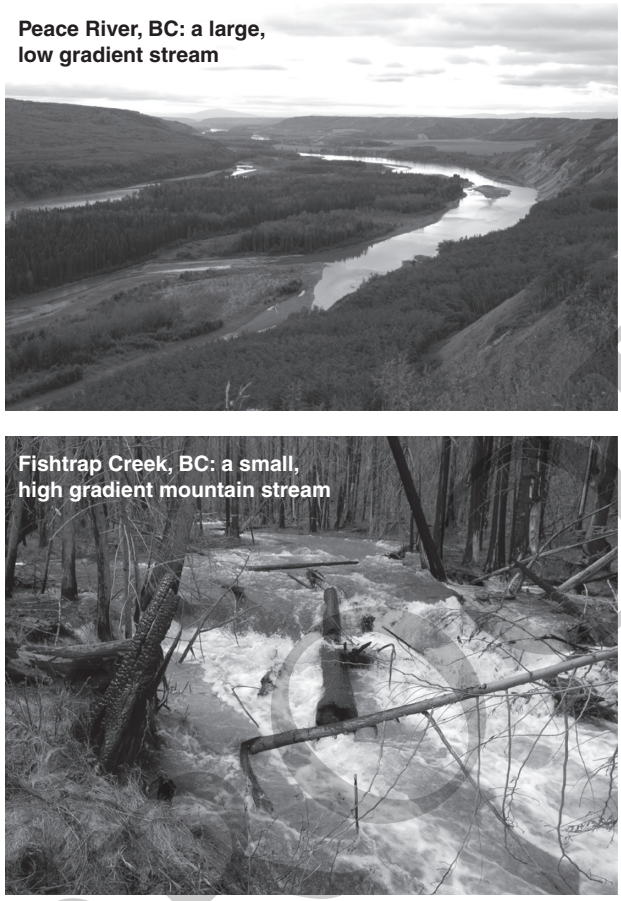

Figure 10.1 Examples of low-gradient and high-gradient streams. The upper panel shows a section of Peace River upstream of Fort St. John, BC in July 2005. The lower panel shows a section of Fishtrap Creek, BC, upstream of the Water Survey of Canada gauge location in May 2007.

hydraulic environment, and highlight their relevance to ecological processes. Our goal is to give students better quantitative tools for describing stream habitats, and a better appreciation of how hydraulics affect ecological processes in streams.

10.2 Hydraulics: The Flow of Water

Our understanding of hydraulics is complicated by spatial and temporal variations in the speed and direction of the flux of water. While water in a stream channel is moving downstream, on average, the flow of water is turbulent, meaning that there can be significant, short-term deviations in the direction and speed of any molecule of water. In order to generate practical, usable equations describing the motion of water, various aspects of this variability have been ignored. As a result, we have different equations for estimating the average flow velocity for a vertical profile taken at a specific point than we

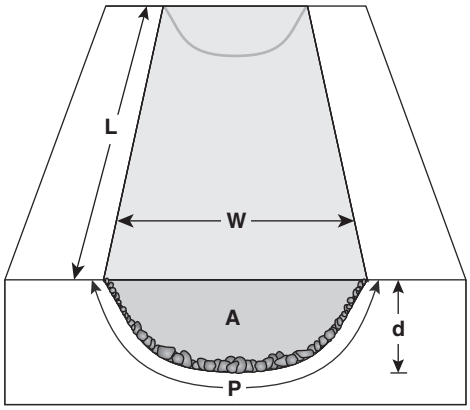

Figure 10.2 Definition diagram for the reference volume of water used to analyze reach-average hydraulic parameters.

do for a reach of river that is several times longer than the channel is wide. It is important for fluvial geomorphologists and stream ecologists to recognize which scale is relevant for a particular problem, and to identify which sets of equations are most relevant.

10.2.1 Reach-Average Hydraulic Relations

At the largest commonly used spatial scale, water flowing downstream is treated in much the same way as a block of wood sliding down an inclined plane, and only the force of gravity (which tends to move water downhill) and the force of friction acting on a reference volume of water (i.e., friction between the "block" of water and the inclined stream bed) are explicitly considered. In Figure 10.2, a reference volume of water is defined by: the **average water surface width, W**, measured perpendicular to the direction of water flow; the **average cross-sectional area of flow, *A***; the average length of the **wetted perimeter, P**, perpendicular to flow; and the **length of the stream reach, L**, in the direction of flow. The force of gravity acting on the reference volume can be expressed using these reach-average parameters as follows:

$$\mathrm{F}_g = g\rho AL \tag{10.1}$$

in which g is the acceleration of gravity (taken to be 9.81 m s^{-1} s^{-1}), ρ is the density of water (typically 1000 kg m^{-3}), and AL represents the reference volume of water upon which gravity is acting. The component of gravity acting parallel to the bed of the river and thereby causing the water to move can be approximated by multiplying F_g by the reach-average **topographic gradient of the channel, *S*.**[1]

[1] Basic trigonometry shows that the downstream component of gravity is F_g sin(β), in which β is the angular inclination of the bed. For small angles, sin(β) ≈ S, the inclination expressed as the ratio of the vertical rise over the horizontal run of the reach. Since river gradients are typically reported as rise over run, sin(β) is virtually never used. The difference between sin(β) and S is less than 1% for $S < 0.14$ m m^{-1}, which includes the vast majority of perennial streams.

A force acting on a mass will accelerate that mass continuously unless opposed by another force. In most streams, the mean velocity tends to remain relatively constant so long as discharge is constant suggesting that, for a given flow, the size of the reference volume adjusts to achieve some kind of balance with an opposing force. For our reference volume of water, the opposing force is due to friction acting on the surface area of the reference volume (given by PL), which is transmitted to the water volume as a shear force. A shear force is one that results from layers of water having different velocities passing over each other. This force balance approach can be used to estimate the **reach-average shear stress, τ_o**, which is the basis for quite a bit of the hydraulic theory that is commonly used. A stress is a force per unit area, so the total shear force acting on the reference volume can be written $\tau_o PL$. It follows that:

$$\tau_o = \frac{g\rho ALS}{PL} \tag{10.2a}$$

which reduces to:

$$\tau_o = g\rho RS \tag{10.2b}$$

by substituting the **hydraulic radius, *R*** (in which $R = A/P$), into the equation. This equation is the basic term that is used to index the average strength of the force exerted by a stream upon its bed. It is the basis for simple estimates of the threshold at which the sediment found in a stream begins to move (where "sediment" refers to all particles ranging from silt to boulders), as well as approximations of the capacity of a stream to transport sediment. It is a fundamental equation that turns up very frequently in fluvial hydrology, because threshold shear stresses for stream bed mobilization and sediment transport have far-reaching effects on channel structure, disturbance frequency, and the hydraulic environment experienced by bottom-dwelling (benthic) organisms like catfish or mayfly nymphs. It should be noted that R is quite similar to the **mean hydraulic depth, *d*** (given by $d = A/W$). In practice, it is common to substitute d for R, giving:

$$\tau_o = g\rho dS \tag{10.2c}$$

This approximation is reasonable, so long as the cross section of flow is relatively wide (i.e., $W/d > 17$). Intuitively, R represents the frictional area (bed surface) available to slow down a given volume of water; increasing the perimeter for a given cross-sectional area should increase drag and slow the volume of water, while increasing the area relative to the perimeter (equivalent to increasing depth) should speed it up.

A simple thought experiment can be used to link this estimate of the force exerted on the stream to the processes controlling the flow of water. Clearly, τ_o depends only on the dimensions of the reference volume (basically, on the mean depth of the flow). The depth of flow is determined by the **stream discharge, *Q***, and the **mean velocity of the flow, *U***. For the same value of Q, a smooth stream channel will allow the water to accelerate to higher speeds than it would in a rough channel, which implies that the

depth of flow in the smooth channel will be smaller than in the rough one. This relation is formalized by the equation for **continuity**, expressed as follows:

$$Q = WdU \tag{10.3}$$

Continuity states that the cross-sectional area for flow (given by the product of W and d) is determined by the stream velocity, U. If Q is constant in the downstream direction (i.e., no tributaries enter the mainstem), then local conditions that cause a 50% reduction in U (say in a deep pool) will result in a 50% increase in the cross section area for flow, with the division between increases in W and in d being determined by the local river topography (i.e., the shape of the cross section). Essentially, Equation 10.3 is used to enforce the principle of conservation of mass.

In order to complete a system of equations for describing reach-average hydraulics, it is necessary to relate the mean shear stress τ_o to the mean stream velocity, U. As the preceding thought experiment suggests, this relation is fundamentally about the roughness of the stream channel. For a given gradient and stream discharge, Q (in $m^3\ s^{-1}$), a rough stream channel will have a low U, a high d and therefore a high τ_o, while a smooth channel will have a high U, low d, and low τ_o. Another way of thinking about this is that, for a given gradient, a water volume will move more slowly only if frictional resistance with the bed is slowing it down and generating high shear stresses at the boundary. Unsurprisingly, this avenue of research has been investigated by using field and laboratory data to empirically relate the ratio of U and τ_o to some relative measure of the roughness of a stream channel bed. In order to make τ_o dimensionally consistent with U, it is expressed as a **shear velocity, u^***, which has the same units as velocity ($m\ s^{-1}$):

$$u^* = \sqrt{\frac{\tau_o}{\rho}} \tag{10.4}$$

and thus,

$$u^* = \sqrt{gRS} \tag{10.5}$$

Researchers have developed a series of empirical equations to predict a dimensionless **flow resistance parameter, Γ,** where $\Gamma = U/u^*$ (see Ferguson, 2007). These empirical functions depend for the most part on the mean hydraulic depth (d) and some measure of the **bed surface roughness**, both of which affect resistance to flow and drag acting on the water column. Using one of these flow resistance laws, U can be estimated as:

$$U = \Gamma\sqrt{gRS} \tag{10.6a}$$

or approximated as:

$$U = \Gamma\sqrt{gdS} \tag{10.6b}$$

in wide shallow channels where R approaches d. The Strickler–Manning equation is a commonly used flow resistance law:

$$\Gamma = a_1\left(\frac{d}{D_{84}}\right)^{1/6} \tag{10.7a}$$

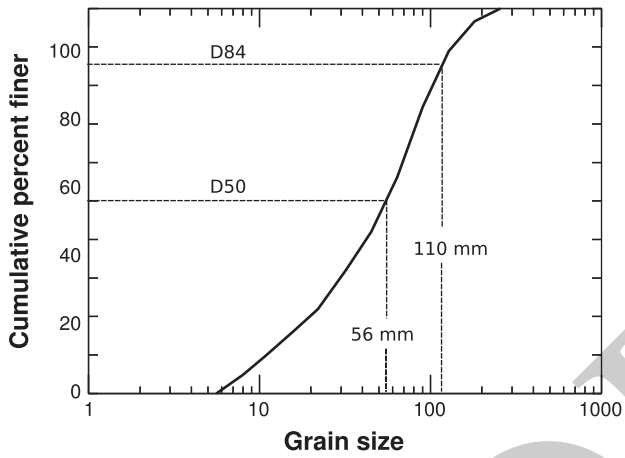

Figure 10.3 An example of a cumulative bed surface grain size distribution. Data come from Fishtrap Creek, BC, which is a gravel bed stream of intermediate size.

In this case, the 84th percentile of the cumulative bed surface grain size distribution, D_{84}, is used as a measure of the bed surface roughness (see Figure 10.3); the larger the grain size, the larger the friction. In the original work by Manning, $a_1 = 8.2$, but a more recent analysis by Parker (1991) indicates that 7.3 is a more reasonable value.[2] This formulation works reasonably well in low-gradient, deep channels, but less well in steep, shallow channels. In those streams, Ferguson (2007) found that flow resistance is better parameterized using a general relation of the form:

$$\Gamma = a_2\left(\frac{d}{D_{84}}\right) \tag{10.7b}$$

where a_2 varies from 1 to about 4. In order to unite these two results, Ferguson (2007) proposed a variable power law formulation:

$$\Gamma = \frac{a_1 a_2 (d/D_{84})}{\sqrt{a_1^2 + a_2^2 (d/D_{84})^{5/3}}} \tag{10.7c}$$

Based on an analysis of the available data, Ferguson (2007) found that values of $a_1 = 6.5$ and $a_2 = 2.5$ produced the best fits.

While Equation 10.7c performs well in gravel and boulder bed streams that have a wide range of gradients and mean depths, it cannot be applied to predict flow resistance in sand bed streams that have beds covered by ripples and dunes, since in these streams the roughness of the bed is due not to the size of the individual grains on the channel bed, but rather to the size of the bedforms that develop on the channel bed. In these streams, it is often necessary to estimate the **characteristic roughness length** (k_s) based

[2] The median surface grain size (D_{50}) is also used to characterize bed roughness, in which case $a_1 = 6.7$.

on measurements of the typical vertical scale of bedforms present, and to use those to parameterize the resistance to flow. This can be done using the Keulegan flow resistance formulation:

$$\Gamma = 2.5 \ln\left(\frac{12.2d}{k_s}\right) \tag{10.7d}$$

If bedforms are not present, then k_s is taken to be the **median bed surface grain size, D_{50}**. Engelund and Hansen (1967) went one step further and presented an approach that can be used to estimate the flow resistance associated with dunes without measuring the dune height directly, but it is beyond the scope of this chapter.

For a stream in which S, $D_{84,}$ and the cross-sectional channel geometry are known, Equations 10.2, 10.3, 10.6, and 10.7 can be used to estimate τ_o and U for any given value of Q. Given that it is both costly and dangerous to make direct measurements of these terms during high flows, this system of equations is a key tool for analyzing the hydraulics of streams.

10.2.2 Cross Section-Averaged Hydraulic Relations

Strictly speaking, Equation 10.2 can only be applied to estimate the average boundary shear stress for a reach that is long enough that local accelerations and decelerations of the flow can be ignored. In order to make estimates of the cross section-averaged shear stress at any point along the length of a stream, we need to consider how energy is stored in a river system, and incorporate all relevant energy terms by replacing the topographic gradient, S, with the **energy gradient, S_o**. If we explicitly include the potential effects of local accelerations and decelerations in the flow, as well as local changes in the mean hydraulic depth, we can apply the reach-average equations above to a given cross section, simply by substituting S_o for S, so long as the changes in U and d in the downstream direction are not too abrupt. Using this approach, it is possible to construct a numerical model (such as the HEC–RAS model developed by the US Corps of Army Engineers), which calculates the longitudinal distribution of τ_o and U within a reach (Brumner, 2010). These one-dimensional hydraulic models are commonly used to estimate the water level at every point along a river for a given flow, and to predict the spatial flooding hazard associated with that flow, or to use point velocity and depth values to infer habitat quality for fish.

In essence, it is the rate at which energy is being lost to the system in the downstream direction that determines the local value of cross section-averaged τ_o. Over a long reach, the total loss of energy is equal to the total drop in elevation over the reach, which represents the loss in **potential energy** for a unit of water ($E'_{pot} = g\rho z$, in which z is the elevation of the channel above some datum). Thus, the topographic gradient, S, can be used as an index of average rate of potential energy loss for a long reach. However, within the reach, there will be zones with lower than average topographic gradient, and higher than average topographic gradient; pools at low flow, for example, may have very little difference in water surface elevation at the upstream and downstream ends, unlike steeper riffles or cascades. Furthermore, there will be systematic adjustments in

both the mean hydraulic depth and the mean velocity, depending on the local topographic gradient. As a result, it is necessary to consider and account for two other sources of energy in the system. The first is the **kinetic energy** possessed by the system ($E'_k = \rho U^2/2$), which is the energy being expended that is capable of transporting sediment and doing work; the second is the energy stored as **hydraulic pressure** ($E'_\psi = g\rho d$). The total energy per unit of water can be written as:

$$E'_{tot} = g\rho z + g\rho d + \frac{\rho U^2}{2} \tag{10.8a}$$

which can be expressed in units of length by dividing each term by $g\rho$, which gives a form of the commonly used Bernoulli equation:

$$H = z + d + \frac{U^2}{2g} \tag{10.8b}$$

The term ***H* is called the total head** and represents all three sources of energy, expressed as a length scale; the term z is referred to as the **elevation head**, representing potential energy; d is the **pressure head**, representing energy stored as pressure; and the last term is called the **velocity head**, representing the kinetic energy of the system.

When stream gradients are reported, there are three potential quantities that can be calculated. The first interpretation ($S = \mathrm{d}z/\mathrm{d}x$) corresponds to the topographic gradient of the channel bed, which is used to represent the reach-average conditions, as described previously. The second interpretation ($S_w = \mathrm{d}[z + d]/\mathrm{d}x$) corresponds to the **topographic gradient of the water surface, $S_\mathbf{w}$**; this is a great improvement over S, and in practice is often used to estimate shear stress within a morphologic unit, such as a pool or riffle. While it is relatively easily to estimate water surface gradient in the field, it still does not represent all relevant sources of energy, since it ignores the velocity head. The final interpretation of gradient ($S_o = \mathrm{d}H/\mathrm{d}x$) includes all of the relevant terms, and is strictly speaking the proper gradient to be entered in any of Equations 10.2, 10.4, and 10.6; it is referred to as the **energy gradient, $S_\mathbf{o}$**. In the field, it is often impractical to estimate U with sufficient spatial resolution to make the calculation of S_o more meaningful than S_w. However, in laboratory settings it is often possible to calculate U at nearly every point along an experimental channel, making it practical to use S_o. Furthermore, numerical models that simulate the longitudinal variations in U and τ_o within a reach are always based on calculated values of S_o. Therefore, S_o is most useful in hydraulic modeling as a concept that fully accounts for all sources of energy. In practice, measurements of the water surface gradient, S_w, are used to estimate U and τ_o at a given location in the field.

10.2.3 Stream Power, Froude Number, and Reynolds Number

There are a number of important metrics that are used to define key attributes in hydraulics that characterize the state of a system. Some of the attributes are dimensional (i.e., associated with units of measurement), including total stream power and unit stream power, and are often used to describe thresholds for river system behavior and

to predict sediment transport rates. Others are dimensionless, and express some basic property of the river system without explicit reference to the scale of the system. These are often used to characterize the dynamic state of a river, or to assess the dynamic similarity of two river systems.[3] These variables are used when developing empirical models of various kinds from field data collected in one or more river systems so that the results can be generally applied to a wide range of streams, regardless of channel scale. They also form the basis for the development of scaled physical models to study prototype river systems.

Stream power: The loss of potential energy per unit length of time ($\Delta E_{tot}/\Delta t$) determines the rate at which geomorphic work (e.g., erosion, sediment transport) can be done by a stream. This is referred to as stream power. In some cases, geomorphologists use the **total stream power** that a river has and in others it is more useful to consider the stream power acting on a 1 m by 1 m area of the bed of the stream, which is called the **unit stream power**. The loss of potential energy per unit length of stream channel is proportional to the change in total head, H:

$$\frac{\Delta E_{tot}}{\Delta x} = mg\frac{\Delta H}{\Delta x} \tag{10.9a}$$

where the mass per unit length of channel, m, depends on the width and mean depth of the river, as well as the density of water (ρ). Given that $S_o = \Delta H/\Delta x$, Equation 10.9a becomes:

$$\frac{\Delta E_{tot}}{\Delta x} = Wd\rho g S_o \tag{10.9b}$$

In order to turn $\Delta E_{tot}/\Delta x$ into a loss per unit rate of time, we simply need to multiply both sides of Equation 10.9b by $\Delta x/\Delta t$, as follows:

$$\frac{\Delta E_{tot}}{\Delta x}\frac{\Delta x}{\Delta t} = Wd\rho g S_o \frac{\Delta x}{\Delta t} \tag{10.10a}$$

which can be rewritten:

$$\Omega = \rho g Q S_o \tag{10.10b}$$

since $U = \Delta x/\Delta t$, and $Q = WdU$. The term Ω denotes the total stream power (W m^{-1}) for a segment of the stream that is 1 m long. This term can be calculated for a stream reach (at which scale $S \sim S_o$) knowing nothing more about a stream than its average topographic gradient and the discharge being conveyed by the stream, Q. If sufficient information exists to make a local estimate of S_o, cross section-averaged estimates of Ω can be made for any point along the length of a stream where S_o is known.

[3] In order to study river system behavior in more controlled circumstances, geomorphologists often build scaled models of river systems in laboratory flumes; the design of such scaled models relies on approximating dynamic similarity while at the same time significantly altering the scale of the system (Peakall *et al.*, 1996).

The stream power acting on a 1m by 1 m area of the channel bed is simply given by dividing Ω by the width of the stream. This is called the unit stream power (ω, in W m^{-2}):

$$\omega = \rho g d S_o U \tag{10.11a}$$

which is equivalent to:

$$\omega = \tau_o U \tag{10.11b}$$

The advantage of ω is that it represents an intensive quantity that allows a comparison between two river systems of different sizes, while Ω is an extensive quantity that is dependent upon the absolute scale of the system, represented by W. The term ω can be estimated for a reach (using S), for a cross section (using S_o), or at any point in the stream (using local measurements of τ_o and U).

Stream power has been used in a number of ways by geomorphologists and ecologists. The concept of stream channel grade, in which the topographic gradient of a stream is adjusted so as to transport the sediment supplied to it with the available discharge is fundamentally rooted in the concept that total stream power determines the capacity of a river to transport sediment (Mackin, 1948; Lane, 1957), and much of the recent work on landscape evolution modeling employs some kind of stream power-based erosion law (e.g., Whipple and Tucker, 1999). Unit stream power has been related to the classification of river channel patterns (e.g., Van den Berg, 1995; Nanson and Knighton, 1996), floodplain types (Nanson and Croke, 1992) and sedimentary bedforms (e.g., Simons and Richardson, 1963); it has also been used to express thresholds for catastrophic channel change during extreme flood events (Magilligan, 1992), and to predict the sensitivity of stream channels to erosion and deposition processes (Bizzi and Lerner, 2013).

Froude number: Froude number is a commonly used dimensionless quantity in hydraulics, which relates the mean flow velocity to the speed at which a gravity wave would move in the stream. The equation for calculating the Froude number (Fr) is:

$$Fr = \frac{U}{\sqrt{gd}} \tag{10.12}$$

The Airy model for **gravity wave** propagation in water (Airy, 1841) predicts that, in shallow water, waves will propagate at a speed given by $(gd)^{1/2}$, so Fr is simply the ratio of the mean velocity at which the medium (i.e., water) is advecting downstream and the speed at which gravity waves can move through the medium.

A gravity wave is generated by, for example, throwing a stone into a pond, wherein the gravity wave takes the form of the ripples migrating away from the point-of-impact. In moving fluids, information about the presence of obstacles protruding into the flow (such as a bridge pier or a large boulder) is transmitted through the flow as a gravity wave as well. When $Fr < 1$, gravity waves propagate upstream at a speed given by $(U - (gd)^{1/2})$, and any obstacles downstream make their presence felt, causing the incoming water to slow down as it approaches the obstacle, and possibly divert around it. This is the principle behind the backwater effect, in which an obstacle placed in a stream can cause water to slow down and back up behind it. Rivers typically exhibit $Fr < 1$, and

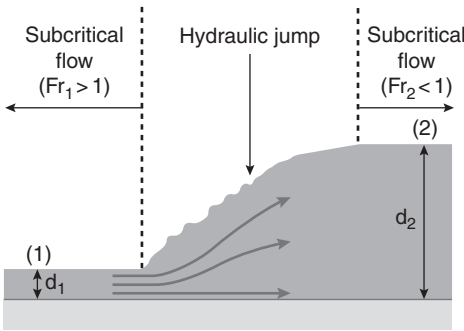

Figure 10.4 A hydraulic jump occurring in a straight flume with constant discharge.

this condition is referred to as **sub-critical flow**. In some circumstances, water may be locally accelerated to the point that $Fr > 1$: this is called **super-critical flow**, and any obstacles in the flow have no effect on the flow of water upstream, until those water particles actually make contact with the obstacle.

Transitions between super-critical and sub-critical flow result in features called **hydraulic jumps** (Figure 10.4). At a jump, the flow transitions from a shallow flow with a very high velocity to a deeper flow with a low velocity. As a result, information about the flow conditions downstream of the hydraulic jump can never be transmitted upstream past a hydraulic jump. The conditions around a hydraulic jump are relatively easily analyzed using the equations that we have already developed. Let us assume that the width of the flow (W) remains constant upstream and downstream of the hydraulic jump. That implies that the **specific discharge** ($q = Q/W$) remains constant[4] as well. Let us make the initial assumption that there is essentially no loss in potential energy across the hydraulic jump, which implies that the **specific energy, *E***, is the same upstream as it is downstream. Specific energy is expressed as a sum of the pressure head and the velocity head:

$$E = d + \frac{U^2}{2g} \tag{10.13}$$

Assuming that d = 0.1 m and U = 1.75 m s^{-1} at point 1 on Figure 10.4, we know that Fr = 1.77, indicating that the flow is super critical. We also know the specific energy, E = 0.26 m, from Equation 10.13. In order to determine what the values are downstream of the jump, it is first necessary to determine how E varies with d for a constant value of q, which in our case is 0.175 m^2 s^{-1}. Substituting q into Equation 10.13 gives:

$$E = d + \frac{q^2}{2gd^2} \tag{10.14a}$$

[4] Discharge has units of m^3 s^{-1}, which means that specific discharge (Q/W) has units of m^2 s^{-1}. Specific discharge can be thought of as the discharge flowing over a 1 m wide section of channel.

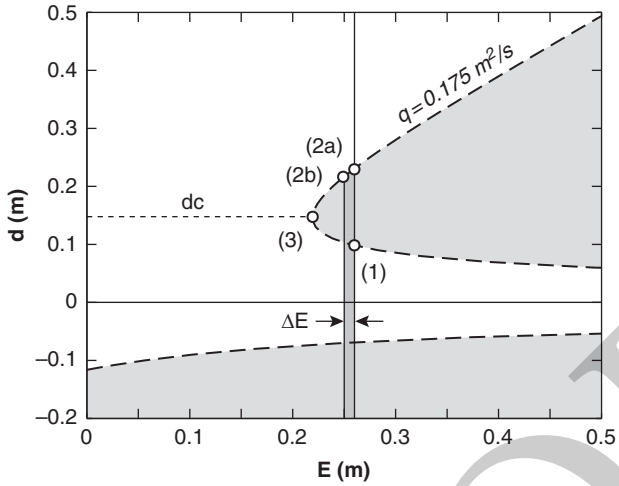

Figure 10.5 Specific energy curve for $q = 0.175\ m^3\ s^{-1}$.

which can be rearranged to isolate the constants on the right hand side, as follows:

$$(E - d)d^2 = \frac{q^2}{2g} \tag{10.14b}$$

This is a cubic equation that has three solutions for a given value of E and q, two of which correspond to sub critical and super critical flows and one of which is invalid, since it is associated with $d < 0$; all three solutions are shown on Figure 10.5. The sub-critical flow (at point 2a, Figure 10.5) with the same value of E is associated with $d = 0.23$ m and $U = 0.76\ m\ s^{-1}$, giving $Fr = 0.51$. If no energy were in fact lost in the transition within the hydraulic jump, then this is the solution value that we would find. However, anyone who has been around a hydraulic jump in the field is aware that water flowing through a jump is very noisy, indicating that at least some of the flow energy is being lost to produce sound.

Indeed, a slight amount of energy is lost in the jump, and a conservation of momentum approach is necessary to accurately predict the flow depth downstream of the jump. Working through conservation of momentum, the depth downstream of a jump is predicted by the conjugate depth equation,[5] shown here:

$$d_2 = \frac{d_1}{2}\left(\sqrt{1 + 8Fr^2} - 1\right) \tag{10.15}$$

By applying Equation 10.15, we predict a depth downstream of the hydraulic jump of $d = 0.21$ m, which is associated with E = 0.25 m, indicating that there has been only a small loss in specific energy (at point 2b, Figure 10.5). This example serves to illustrate

[5] The derivation of this equation can be found in most standard textbooks on the hydraulics of open channel flow (e.g., Henderson, 1966).

that hydraulics are predictable, but that both conservation of energy and conservation of momentum must be considered. It also clearly indicates that for almost all combinations of E and q, there are two combinations of d and U that satisfy conservation of specific energy, corresponding to the sub-critical and super-critical flow conditions. The exception to this occurs at the local minima of E, where $dE/Dd = 0$, at which point only a single solution exists. The flow at this point is said to be **critical flow**, and $Fr = 1$. The depth at which the flow reaches the critical depth, d_c is given by:

$$d_c = \left(\frac{q^2}{g}\right)^{1/3} \tag{10.16}$$

In our example, $d_c = 0.146$ m, giving $U = 1.20$ m s^{-1} and of course $Fr = 1.0$.

The Froude number characterizes a river system with respect to forces and phenomena associated with gravity forces, which includes the transitions in flow that occur at hydraulic jumps, flow constrictions, and weirs and sluice gates. These transitions are often associated with falls or other vertical drops that may act as barriers to upstream migrating fish. Even without vertical drops, super-critical velocities may make fish passage difficult, and the deeper sub-critical flow below a hydraulic jump may be essential for salmon and trout to build enough speed to jump over and swim upstream of weirs or falls.

Reynolds number: The Reynolds Number (*Re*) is a dimensionless ratio of the inertial forces and the viscous forces in the flow. Inertial forces are what tend to keep objects moving once they are in motion, whereas viscous forces in a fluid tend to dampen turbulence. The equation used to calculate *Re* is:

$$Re = \frac{\rho U d}{\mu} \tag{10.17}$$

in which μ is the **molecular viscosity** of the fluid. The numerator represents a measure of the inertia of the flow, averaged over the mean hydraulic depth, while the denominator represents the viscous forces within the flow. When the inertial forces are small relative to the viscous ones, the flowing fluid will exhibit no vertical mixing such that fluid near the bed will stay near the bed, while fluid near the surface will stay there. In this circumstance, shear forces are transmitted between layers of fluid moving in the downstream direction simply via viscous interactions between the fluid molecules, and the flow is said to be **laminar**. This generally occurs when $Re > 500$, which corresponds to very shallow, slow moving flows. For $500 < Re < 2000$, the flow may develop eddies around an obstacle in the flow which introduce complex (but not chaotic) oscillations in flow magnitude and direction. Such flows are sometimes called **transitional**, but are also very rare in natural streams.

Turbulent flows are typically associated with $Re > 2000$, which is the case for virtually all flows of interest to the natural scientist. When the inertial forces are much greater than the viscous ones, the inertia of moving water in different vertical layers will produce turbulent eddies, resulting in significant vertical mixing within the water column as eddies transfer slow moving parcels of water away from the channel bed

and bring fast moving water towards it, intensifying the vertical velocity gradient relative to laminar flow. While the instantaneous magnitude and direction of flow of any molecule of water in the flow is chaotic, the time-averaged distribution of velocities with the flow is organized in a way that is qualitatively similar to the velocity distribution in a laminar flow. However, the instantaneous forces are significant both for the entrainment and transport of sediment within the stream and to the nature of physical habitat for fish and benthic invertebrates, so turbulence is a significant attribute that influences many riverine processes.

Reynolds particle number: Another kind of Reynolds number is used to describe the flow conditions close to the bed of the stream channel, and is called the Reynolds particle number, Re^*. It is essentially the same as Re, but it is used to represent flow conditions near the bed of the stream channel, rather than the conditions averaged over the scale of the flow depth. In this case, the scale of reference is reduced to that of the diameter of the particles on the bed, D. The inertial forces in the vicinity of the bed are related to the velocity around the particles, and are represented using the shear velocity, u^*. Making these two substitutions into Equation 10.16, the equation for estimating Re^* becomes:

$$\mathrm{Re}^* = \frac{\rho u^* D}{\mu} \tag{10.18}$$

As a matter of convention, it is common to substitute the **kinematic viscosity, v** (which is defined as $v = \mu/\rho$), when writing Equation 10.18, but doing so merely obscures the fact that the only significant difference between Equations 10.17 and 10.18 is the spatial scale over which the inertial forces are computed. Re^* is used primarily to distinguish between hydraulically rough flows, in which the particles on the channel bed protrude above the thin zone of laminar flow that must exist close to the channel boundary, from hydraulically smooth flows, in which the particles are contained within a thin layer of laminar flow. The zone in which the flow is laminar is called the **laminar sub-layer**, and the thickness of this layer, δ, is estimated as follows:

$$\delta = \frac{11.5v}{u^*} \tag{10.19}$$

When $Re^* > 70$, then the flow is said to be **hydraulically rough**; based on Equation 10.19, this corresponds to a situation in which $D > 6(\delta)$. **Hydraulically smooth** flows are associated with $Re^* < 3$, which corresponds to $\delta > 4(D)$. For $3 < Re^* < 70$, the flow is **transitional** between turbulent and laminar conditions. Whether or not a flow is hydraulically rough, smooth, or transitional has a strong influence on the flow conditions required to entrain and move the bed sediment, which is discussed in Section 10.3.

10.2.4 Velocity Profiles and Flow Separation

So far, we have addressed the means by which average channel velocity is defined and estimated. However, at a single location across the stream, velocity varies systematically

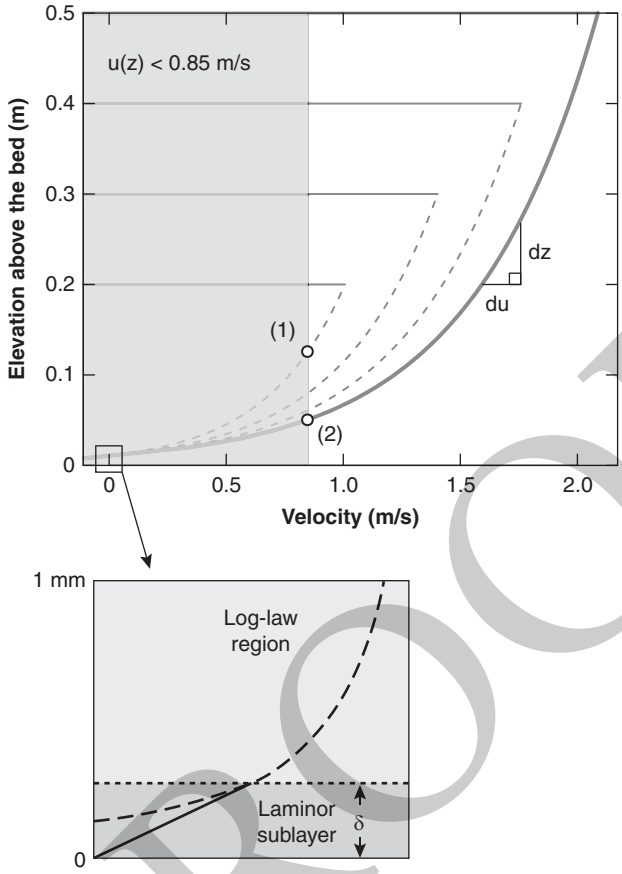

Figure 10.6 Velocity profiles for various flow depths defined using the log law of the wall, using k_s = 128 mm and S_o = 0.01 m m^{-1}. The typical scale of the laminar sublayer is indicated in the inset schematic diagram.

with distance from the stream bank and elevation above the bed. The variation of velocity with distance above the stream bed is called a **velocity profile**. The water flows most slowly near the bed because of friction with the substrate, and increases with distance from the boundary until it reaches the **mean free velocity**. The region where the velocity gradient is steepest is called the **boundary layer**, and this is where shear stresses are generated. In many streams where the flows are relatively shallow, the boundary layer extends right to the surface of the water, and the flow never reaches the mean free velocity (Figure 10.6).

Within the boundary layer, the velocity profile (i.e., the distribution of velocity with height above the bed) generally follows the **log law of the wall**:

$$u(z) = \frac{u^*}{\kappa} \ln\left(\frac{z}{z_o}\right) \tag{10.20}$$

in which κ is **von Karman's constant** ($\kappa \approx 0.4$), z is distance measured upwards from the bed surface, u^* is the shear velocity,[6] which is related to the diffusion of momentum from the flow towards the bed, and z_o is the height above the bed at which $u(z) = 0$ m s^{-1}. This equation is directly related to the flow resistance law discussed earlier (Equation 10.7d). The term z_o is directly related to the size of the sediment found on the bed. The larger the substrate size, the greater the flow resistance, and the thicker the boundary layer. For a gravel bed, $z_o = D_{84}/12.2$, typically.

As the total depth of the flow increases, the velocity gradient near the bed becomes steeper such that u^* increases too (Figure 10.6). Let us assume that some particular species of fish is unable to hold its position in water flowing faster than 0.85 m s^{-1}; for a total flow depth of 0.2 m, Equation 10.20 predicts that velocity will be less than 0.85 m s^{-1} only for $z < 0.12$ m, but as the water depth increases to 0.5 m, $u(z) < 0.85$ m s^{-1} only for $z < 0.05$ m, indicating that the area of available habitat for our species of fish has been potentially cut in half (see Figure 10.6).

Both the velocity profile and substrate size are key habitat features that affect the distribution of stream organisms and the range of habitats that are usable for any species (or size class – because small fish cannot swim as fast as larger ones, habitat requirements often differ by life stage). As the preceding example illustrates, if water velocity is too fast then fish cannot exploit habitat above the substrate. As a consequence, one of the most fundamental adaptations of many species is to become benthic (bottom-dwelling), which allows organisms to exploit habitats where velocities are too fast for fish that swim in the water column (Figure 10.7). A benthic lifestyle allows fish to minimize swimming costs by resting directly on the stream bed while preying on benthic invertebrates (e.g., mayfly nymphs, stoneflies, chironomids) or other fishes in the velocity refuge associated with coarse bottom substrate. Benthic fish species include suckers, sculpin, and catfish, some of which have adapted to the extent that they have lost their swim bladders (an internal gas-filled organ to maintain buoyancy) over evolutionary time. While some benthic species occur in deeper habitats like pools where shear stress is low, others occur in high velocity reaches with powerful shear forces, but with roughness elements such as cobbles and boulders, which create a hydraulically benign environment that benthic fish can exploit (Figure 10.7).

Drift-foraging fishes like salmon and trout that hold in the water column and feed on invertebrates floating by in the current have contrasting vulnerabilities and requirements to benthic fishes. Turbulence in particular can affect habitat selection by drift-feeders, since directional changes in water velocity and acceleration in turbulent flow greatly increases swimming costs (Enders *et al.*, 2003), and likely degrades prey capture success (Rosenfeld *et al.*, 2014). Although drift-feeding fish may have difficulty feeding effectively in the main flow of a very turbulent river, trout and salmon have been shown to preferentially select slow-velocity microhabitats (e.g., behind

[6] In this case, u^* must be calculated for the point at which the velocity profile is collected (i.e., using local estimates of d and S_o), not using cross section-averaged inputs. In fact, in practice Equation 10.20 is most often used to estimate u^* at a given point by fitting the log law of the wall to data from a velocity profile.

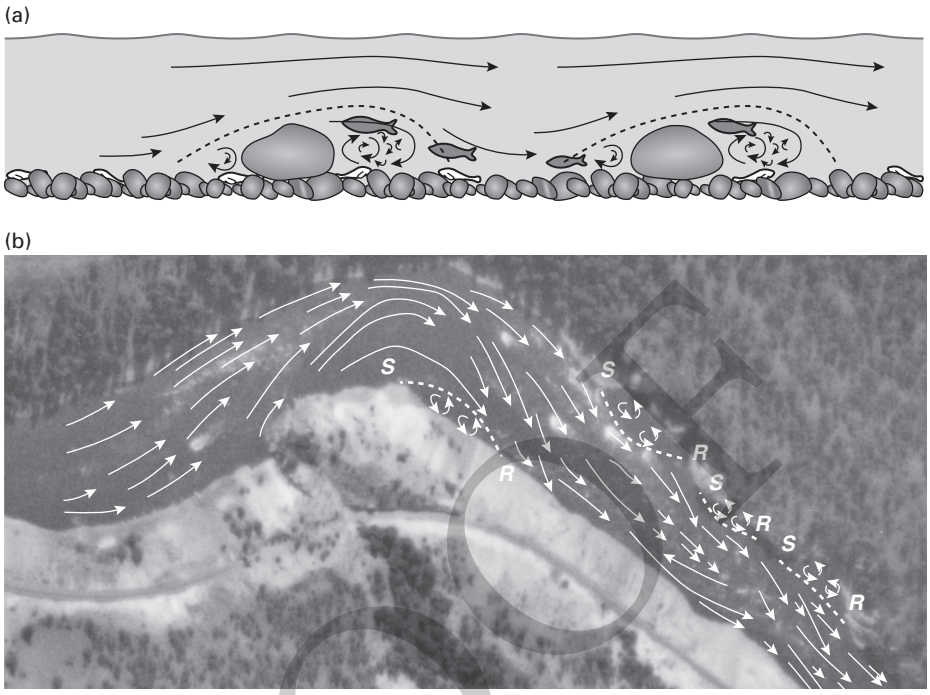

Figure 10.7 Flow separation at: (a) obstacles protruding into the flow, and (b) sharp bends in the stream channel bank alignment: in this figure, the point at which the boundary layer separates from the channel bank is labeled (S), as is the point at which it becomes reattached (R). Dark fish represent drift-feeders like trout that swim in the water column, and exploit flow separation to reduce swimming costs behind larger obstacles in high-velocity reaches. Smaller benthic (white) fish can exploit lower velocities closer to the bed and be more broadly distributed.

logs or boulders) adjacent to high-velocity gradients (Hayes and Jowett, 1994), which allows them to scan a large volume of flowing water for drifting prey while minimizing their swimming costs.

Not only do obstructions provide flow refugia that reduce velocities and swimming costs for drift-feeding fishes, recent studies have also shown that fish actively use the turbulent eddies shed at the edges of obstructions to achieve upstream propulsion, thereby greatly reducing their swimming costs at a fixed focal point (Liao *et al*., 2003a, 2003b; Taguchi and Liao 2011). Similarly, scientists using radiotelemetry to measure tail beat frequency of migrating salmon have shown that upstream migrants may travel faster than they should based on their rate of muscle contraction, indicating that fish can take advantage of small- to medium-scale turbulence structures (e.g., upstream eddies) to hitch a ride and reduce their swimming costs (Hinch and Rand, 2000).

This discussion highlights the pervasive importance of velocity profiles and shear forces to habitat selection, foraging success, community structure, and ultimately production of stream fishes. While the stream community will respond primarily to the emergent properties of the velocity profile, the composite processes that generate the profile bear closer examination. The force that acts on the bed at a given discharge

depends on how quickly momentum is being diffused towards the bed from the flow. In flowing water, forces are transmitted between molecules that slide over each other but which exhibit some molecular attraction or "stickiness," which is what the molecular viscosity of a fluid represents. The force of gravity acting to pull water down the slope is transmitted diffusively from molecule to molecule until it is ultimately transferred to the bed of the stream, but an additional process that contributes to the shear force acting on the bed is the convective transfer of momentum within the flow due to turbulence: the first process is indexed by the **molecular viscosity of the fluid, μ**, and the second is indexed by a term called the **turbulent viscosity, η**. In fact, shear stress can be defined at any point within the velocity profile as follows:

$$\tau(z) = (\mu + \eta)\frac{du}{dz} \tag{10.21}$$

Based on this re-definition of shear stress, it should be evident that the size of the force acting on the bed depends on the combined molecular and turbulent viscosities and how fast the molecules are moving past each other. However, it is difficult to predict the value of η for a given flow, and its value actually changes in some parts of the boundary layer. Therefore, if we wish to estimate the shear stress acting on the bed at a given velocity profile, τ_i, it is more convenient to make use of Equation 10.20 than it is to try and estimate η. By measuring the velocity profile at a given point, we can fit Equation 10.20 to the data and use the statistical fit to estimate the shear velocity, u^*. Then we can estimate the local shear stress, τ_i, since $\tau_i = \rho u^{*2}$. In this way, we could in theory estimate τ_i at a large number of places within the channel for a given flow, and then map the distribution of shear forces acting on the bed of the channel. This is seldom possible, given the difficulty of collecting enough data before flows change. While this kind of detailed information on the forces acting on the channel bed is highly desirable, fluvial geomorphologists often have to settle for estimates of the average shear stress acting on the channel boundary, τ_o, which are more easily obtained.

Flow separation occurs around obstacles that protrude into the flow or at sharp bends in the alignment of the stream banks. For an obstacle that protrudes into the boundary layer, the pressure exerted on the flow propagates upstream, slowing the incoming water. At the separation point, the water at the bed actually stalls, such that the incoming water is forced up and over the obstacle, resulting in a boundary layer that is separated from the stream bed by a zone in which water trapped by the obstacle recirculates (Figure 10.7a). The boundary layer may also be separated from the top of the obstacle by a small zone of recirculation, and it re-attaches with the bed well downstream of the obstacle, producing the largest zone of recirculation immediately downstream of the particle. These zones of separated flow scale with the size of the obstacle, and can act as important, low energy refugia for benthic invertebrates and some species of fish (Figure 10.7a). They are also zones where finer than average sediment can be trapped and deposited. A similar phenomenon occurs at the channel banks, but on a different spatial scale (Figure 10.7b). Where sharp changes in bank orientation occur, the flow can separate from the channel banks, producing large zones of recirculating flow with dimensions on the order of the channel depth. These may also be ecologically important

low energy refugia for resident or migratory fishes, and they may also trigger deposition of inorganic sediment and organic detritus.

The ecological significance of low-velocity marginal and lateral habitat cannot be overemphasized. These areas of flow separation are particularly important for larval salmon and trout immediately after they have emerged from the gravel, when their limited swimming ability makes them dependent on shallow, marginal, slow-moving habitat in steep gradient trout streams (Moore and Gregory, 1988; Armstrong and Nislow, 2006). Drifting prey are also delivered into these hydraulically sheltered stream margins by turbulent bursts of water intruding from the main body of flow across the zone of flow separation. If lateral circulation cells are large enough (e.g. Figure 10.7b), juvenile trout can often be observed drift feeding while swimming into the current in a downstream direction in lateral habitat. Low-velocity circulation cells are also important zones of terrestrial organic matter deposition, storage, and processing by aquatic invertebrates that consume detritus (e.g., tree leaves) at the base of aquatic food webs (Allan and Castillo, 2007).

10.3 Morphodynamics: Channel Structure and the Flow of Sediment

Up to this point, we have been dealing almost exclusively with the movement of water over a fixed, immobile bed. Of course, the boundary in most rivers is not immobile and indeed has been shaped by the water flowing over it. An important component of any fluvial system is the sediment flowing downstream, as well as the water. Unfortunately, a complete, physically based theory of sediment transport in river systems remains elusive. The situation is further complicated by wood, which is commonly present in forested streams and also affects the movement and deposition of sediment.

Generally, the sediment entering a stream can be categorized by the way in which it moves (Figure 10.8). The smallest sediment sizes (silts and clays) are carried in **suspension** in nearly all stream channels. In steep streams, these sediment sizes can be transported through a reach of a river without being deposited at all. In channels with low gradients, a fraction of the incoming silt and clay may be trapped in low energy zones, particularly when flood waters carry them out of the main channel and onto the adjacent floodplain. Generally, these sediments form the upper part of a stream bank for many streams. The larger sediment sizes, including gravel, cobbles, and boulders are transported in **traction**, which involves rolling, sliding, or bouncing along the bed of the stream. These sediment sizes form the bulk of the material found within the active stream channel (called bed material). The intermediate grain size, sand, can move either in suspension or in traction; it can also move in a series of ballistic hops of considerable length, a kind of movement referred to as **saltation**. It is often the case that sand will move in traction at low flows, but will then either saltate or be suspended as turbulence increases at higher flows. Sand is found in appreciable quantities both in the bed material found in the active stream channel and in the finer sediments deposited upon the floodplain (Figure 10.8).

A stratigraphic section through the floodplain of a gravel bed river will reveal gravel, cobbles, and possibly boulders in the lower part of the section, the deposition of which

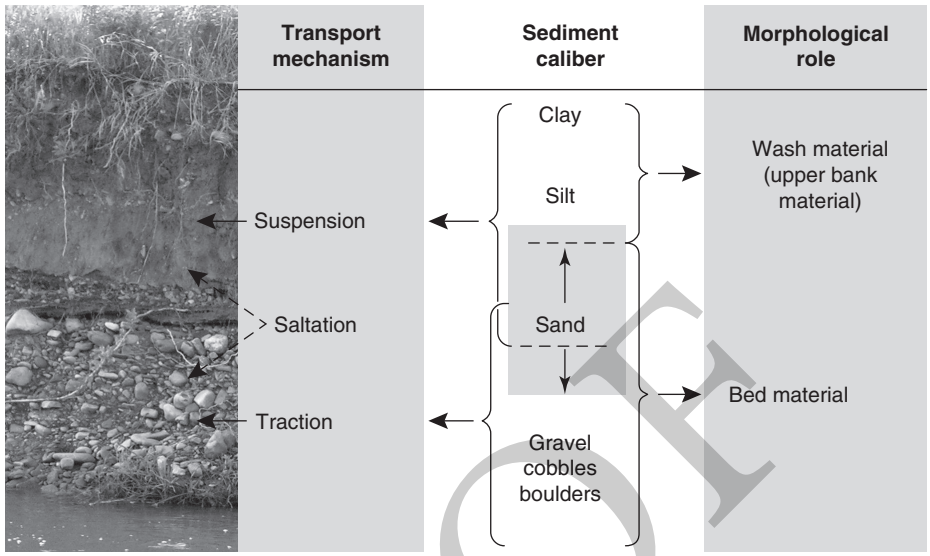

Figure 10.8 Schematic diagram indicating typical transport mechanism and morphological role for various grain sizes in transport (after Church, 2006).

is associated with the migration of the channel across its floodplain, and finer sediments (including sand, silt and possibly clay) in a layer above that (Figure 10.8). The deposits in the upper layer are associated with suspended sediment carried out of the main channels during floods, where it encounters increased flow resistance due to vegetation on the top of stream channel bars and on the floodplain, slowing the water and permitting these finer sediments to deposit out of suspension. These deposits also provide the basic building blocks for the development of a soil that can support a wide variety of vegetation, and thus are part of a feedback system in which the geomorphic system and the riparian ecosystem act upon each other (Hickin, 1984).

In many fluvial systems, sediment transport of the bed material only occurs during relatively rare high-flow events. In fact, early work by geomorphologists suggests that many characteristics of a stream channel can be associated with what is called the **bankfull discharge** (Leopold and Maddock, 1953; Leopold and Wolman, 1957; Wolman and Miller, 1960). Bankfull discharge refers to the flow that is just sufficient to fill the stream channel without spilling out onto the floodplain adjacent to the stream. Figure 10.2 is a schematic diagram representing the bankfull condition for a highly idealized stream channel, while the lower panel of Figure 10.1 shows a stream at bankfull flow. Typically, rivers will reach the bankfull flow once every one or two years, though bankfull flows can be much rarer in arid regions. Flows at (or close to) the bankfull level generally do more geomorphic work (in terms of cumulative transport of sediment and reshaping the channel) than smaller, more frequent flows and larger, less frequent ones (Benson and Thomas, 1966; Pickup and Warner, 1976; Andrews, 1980; McLean *et al.*, 1999), which underlines the significance of this reference flow for understanding stream channel dynamics. Nevertheless, sediment transport at lower

flows can still be of ecological consequence. For instance, Luce *et al.* (2013) found that significant scour of algae growing on rocks can occur at flows well below bankfull, and that algae on low-lying rocks was more vulnerable to abrasion than on rocks that protruded higher into the water column, and were less exposed to saltating particles.

10.3.1 Incipient Motion and Settling Velocity

The processes controlling the **entrainment** of sediment by water are relatively well understood, and we commonly analyze the threshold for entrainment using the median grain size of the bed surface (D_{50}), but researchers have also developed equations to predict the movement of particles of any arbitrary size found on the bed surface, D_i. For a flow that is at the entrainment threshold for the D_{50}, those particles that happen to be highly exposed to the flow by virtue of their position on the bed will be moved first. These are the particles that are not partially buried by other particles, that are relatively exposed (rather than hiding in the zone of recirculation behind a larger particle, upstream), and whose movement is unencumbered by the particles in physical contact with it. A simple force balance argument is used to set up the problem, but the threshold of entrainment has been determined empirically through a series of laboratory experiments and field observations. The main force resisting particle movement is assumed to be proportional to the submerged weight of the particle $\left(F_{resisting} \propto g(\rho_s - \rho)D_{50}^3\right)$, in which ρ_s is the density of the sediment. The main force driving entrainment of the particle by the flow is assumed to be proportional to the total shear force acting on the particle $\left(\mathrm{F}_{entrainment} \propto \tau_o D_{50}^2\right)$. Experiments to measure the entrainment threshold have determined the shear stress at which $F_{entrainment}$ equals $F_{resisting}$ and studied the behavior of a constant of proportionality, θ_c, which is called the **critical Shield's number**, after the original author of this approach. The basic model representing our understanding of the entrainment process can be written:

$$\tau_{c50} = \theta_c g(\rho_s - \rho)D_{50} \tag{10.22}$$

in which τ_{c50} refers to the empirically observed boundary shear stress at which the D_{50} is first entrained by the flow. Shield's work was conducted with sediment of uniform size, and he found that, so long as $Re^* > 70$, θ_c was basically constant, having a value somewhere between 0.03 and 0.06 (Figure 10.9).

For entrainment of sediment from a stream with a mix of sediment sizes, various researchers have confirmed that the median grain size of the surface (D_{50}) behaves much the same as the unimodal sediments in Shield's original experiments, being entrained when $0.03 < \theta_c < 0.06$ (Andrews, 1983; Carling, 1983; Komar, 1987). Research by others has identified a number of reasons for this variability, including: the shape of the particles (round ones are more easily entrained than flat ones); the structural arrangement of the bed (beds that are loosely structured with lots of open pore spaces are more easily entrained than highly compacted and imbricated beds); and the percent of fine material on the bed (once the percent of sand in a gravel bed rises above about 30%, gravel is more easily entrained than if the sand were absent). A reasonable value for most gravel beds is somewhere in the middle of the range ($\theta_c = 0.045$), but it is

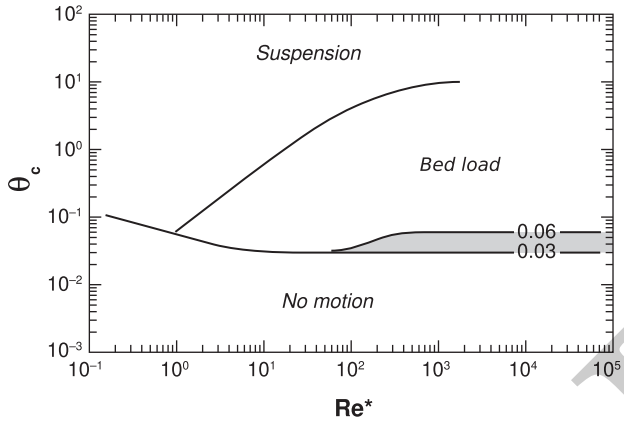

Figure 10.9 Thresholds for particle entrainment and particle suspension.

important to remember that significant scatter exists in the estimates of θ_c. When the bed surface is highly structured such that many of the grains are interlocking, making entrainment much more difficult, a reasonable value for θ_c might be as high as 0.09. It is also worth keeping in mind that entrainment occurs during the highest instantaneous shear stresses associated with strong turbulent eddies impinging on the stream bed, and that the time-averaged boundary shear stresses estimated using the equations above are merely proxies for these higher instantaneous shear stresses.

For $Re^* < 3$, the influence of the laminar sublayer (discussed earlier in this chapter) at the boundary becomes increasingly significant, making it relatively more difficult to entrain particles on the bed. As shown in Figure 10.9, the coefficient θ_c increases monotonically as Re^* decreases below 3 to a maximum of about $\theta_c = 0.1$. This behavior reflects the fact that, as the thickness of the laminar sublayer becomes large relative to the grain size diameter, it becomes increasingly difficult for high-energy turbulent eddies to reach the stream bed and entrain sediment.

Once the shear stress exerted on the bed exceeds the critical shear stress for the D_{50}, the particles of that size begin to show up in measurements of the sediment being transported by the stream, but most of the sediment being transported will be finer than that because small particles have lower thresholds for entrainment. In fact, the proportion of sediment in the D_{50} size class found in the sediment being transported (called the **sediment load**) will be much lower than the proportion of sediment on the stream bed in that size class. When the proportion of sediment in a given size class being transported is much less than the proportion on the bed surface, that fraction is said to be **partially mobile** (after Wilcock and McArdell, 1993). Once the shear stress exerted on the bed exceeds about two times the shear stress required for entrainment for a given particle size, the particle size class becomes **fully mobile**, meaning that the proportion of the sediment load in that class is effectively the same as the proportion of the bed surface in that size class.

One consequence of the lower critical shear stress of smaller particles is that they are transported during a much wider range of flow conditions than larger ones, resulting in a

coarsening of the stream bed surface relative to the sub-surface particle size distribution. This results in bed armoring, where the coarser surface substrate particles protect subsurface particles from downstream transport (Parker and Klingeman, 1982).

While it is clear from empirical studies that different particle sizes are entrained from a bed at different shear stresses (i.e., smaller particles on the bed start moving at lower shear stresses than larger ones), the differences are smaller than would be predicted from Shield's original experiments using unimodal sediment. For particles that are smaller than average, the value of θ_c increases, while for larger than average particles, it decreases. In fact, in many gravel bed streams, sediment transport is most strongly influenced by the mobility of the D_{50}, such that nearly all particles begin to move at close to the same shear stress (Parker and Klingeman, 1982). The entrainment threshold of grains of size D_i from a bed having a median surface size of D_{50} is typically expressed using a power function of the form:

$$\frac{\tau_{ci}}{\tau_{c50}} = \left(\frac{D_i}{D_{50}}\right)^b \tag{10.23}$$

in which τ_{ci} is the boundary shear stress required to entrain particles of size D_i, τ_{c50} is the shear stress required to entrain the D_{50} (which can be estimated using Equation 10.22), and b is an exponent; Wilcock and Crowe (2003) suggest that for $D_i < D_{50}$, b is about 0.12, but that for $D_i > D_{50}$, b is about 0.67, indicating that an incremental increase in shear stress will mobilize a much larger proportion of the particle size distribution below D_{50} than above it. As an example, consider a bed with a surface distribution such that the upper quartile of the distribution is 100 mm, the median is 50 mm, and the lower quartile is 25 mm. Assuming, as is commonly done, that $\theta_c = 0.045$, $\rho = 1000$ kg m^{-3}, and $\rho_s = 2650$ kg m^{-3}, the D_{50} would be predicted by Equation 10.22 to begin moving at a shear stress of about 36 Pa. Using Wilcock and Crowe's (2003) values in Equation 10.23 predicts that the lower quartile would begin moving at 33 Pa, whereas the upper quartile would begin moving at 58 Pa, which is a reasonably narrow range of shear stresses.

This example is also useful for illustrating the distinction between partial mobility and full mobility. Consider the 100 mm particle described previously: it is a larger than average grain, producing a flow separation zone behind it that could represent an important habitat element for benthic invertebrates and various species and life stages of fish. Virtually all of these grains are likely to remain stable for flows generating less than 58 Pa, even when the surface D_{50} (and all of the sediments finer than that) are being entrained. For flows generating shear stresses between 58 Pa and 116 Pa, 100 mm particles will become partially mobile, and some of them will begin to move. At the low end of this range, only the most precariously positioned particles will be entrained, with most remaining stable, meaning that most of the available habitat will be relatively unaffected. Once shear stresses exceed about 116 Pa, the full mobility threshold is crossed and effectively all particles of this size will be entrained by the flow, meaning that any habitat value provided by these sizes of particles will be lost. Fortunately, while it is common for the D_{50} to become fully mobile at flows approaching the bankfull flow, it is much less common for the largest grains on the stream bed to become fully mobile (Haschenburger and Wilcock, 2003).

Entrainment and transport of sediment presents an adaptive challenge to organisms in running waters (Hynes, 1970; Allan and Castillo, 2007), which have evolved various adaptations to minimize the likelihood of being washed downstream. For example, the endangered Sonoran Desert topminnow is rapidly extirpated through predation by introduced mosquitofish (Meffe 1985) in streams with stable flow regimes; however, behavioral adaptations of the topminnow to avoid displacement during flash floods allow the two species to coexist in more flashy streams because mosquitofish (which have not been selected to detect cues of approaching flood crests) are periodically decimated. Nevertheless, there are limits to adaptation, and catastrophic flood events that mobilize the entire stream bed may result in scour, downstream displacement, or mortality even of co-adapted fishes and invertebrates (Roghair *et al.*, 2002; Pujolar *et al.*, 2011).

There is another threshold to be considered in addition to entrainment. At higher flows, the upwards-directed component of turbulent fluctuations can be sufficient to lift particles up into the flow and to keep them suspended there for extended periods of time. **Suspension** occurs when the velocity at which a grain would fall through a still body of water (called the **settling velocity**, u_s) is equal to the shear velocity, $u*$, given by Equation 10.4; in this case, u^* acts as a proxy for the intensity of the turbulence in the flow. The suspension threshold calculated in this way is plotted on Figure 10.9. Note that, when very small particles are entrained, they are pulled out of the laminar sublayer and immediately exposed to the more energetic turbulent boundary layer where they immediately move in suspension, supported by turbulent eddies in the water column. When larger particles are entrained by the flow, they move in traction along the bed, rolling, sliding, and bouncing, but primarily in contact with the bed itself, only moving into suspension at exceptionally high flows. Practically speaking, silt- and clay-sized particles move predominantly in suspension, sand-sized particles commonly move both in suspension and in traction, while particles larger than sand are almost never subject to flows sufficient to suspend them.

The settling velocity can be derived by constructing a simple force balance between the force of gravity and the drag force generated by the relative motion between the particle and the fluid through which it is falling. The drag force acting on a spherical particle with radius r is given by $F_{drag} = CD\pi r^2 \rho u^2/2$, in which C_D is the drag coefficient and u represents the relative velocity between particle and fluid. The effective force of gravity for a spherical particle (accounting for the submerged weight of the particle) is given by $F_{gravity} = (4/3)\pi r^3 g(\rho_s - \rho)$. At the steady-state settling velocity, $F_{drag} = F_{gravity}$ and we can solve for u_s:

$$u_s = \sqrt{\frac{4g(\rho_s - \rho)D}{3\rho C_D}} \tag{10.24a}$$

In this version of the equation, we have substituted D for r. This version of the equation works reasonably well for larger particles (D larger than about 3 mm) which fall faster, and have a coefficient of drag that does not vary with particle size, but remains constant at a value of about 0.44. For smaller particles ($D < 0.1$ mm), C_D varies predictably with

the Reynolds number that characterizes flow around the particle,[7] and the settling velocity can be calculated using the Stokes settling law:

$$u_s = \frac{g(\rho_s - \rho)D}{18\mu} \tag{10.24b}$$

In order to avoid the necessity of using two equations and to improve the accuracy of the settling law for non-spherical particles, Ferguson and Church (2004) developed a universal settling law that can be used for all particle sizes:

$$u_s = \frac{sgD^2}{C_1\mu/\rho + \sqrt{0.75C_2 s_g D^3}} \tag{10.25}$$

This equation numerically approximates the two solutions derived from first principles (Equations 10.24a and 10.24b). The constant s is the submerged specific gravity of the sediment ($s = \rho_s/\rho - 1$), and the coefficients C_1 and C_2 are empirically derived values that depend weakly on particle shape. For sands, Ferguson and Church (2004) recommend setting $C_1 = 18$ and $C_2 = 1.0$.

Although the processes of entrainment and settling are fundamental to inorganic sediment transport, they are also important for the dynamics of invertebrate drift, which is the process whereby benthic invertebrates enter the water column to be transported downstream. Drift may be initiated through deliberate behavior to redistribute while foraging or to avoid benthic predators (Kohler, 1985; McIntosh and Townsend, 1998), or drift may be the result of high shear stresses (often associated with periodic turbulence events; Blanckaert *et al.*, 2013) and/or substrate mobilization during a flood (Gibbins *et al.*, 2007). Although settling rates of invertebrates remain poorly understood, active swimming behavior allows invertebrates to settle more quickly than particles, or to remain in suspension if desired; for example, mayfly nymphs will spread their legs and parachute to increase drag to keep in suspension (McIntosh and Townsend, 1998), while other aquatic insect larvae like *Hydropsyche* caddisflies may cannonball (curl up into a ball) to reduce drag and settle more quickly (Hauer *et al.*, 2011).

Another key element in stream channels in forested environments is the large wood that is supplied to stream channels from the surrounding riparian forests. Large wood (LW) can interact with the transport and storage of bed material in stream channels, provide cover for aquatic organisms, and form other important habitat elements. Generally, researchers have found that the entrainment of a piece of wood depends on the density of the wood and the piece diameter (Braudrick and Grant, 2001) and the mode of movement, which can be classified as either rolling or sliding (Bocchiola *et al.*, 2006). Generally speaking, LW can be entrained when the ratio of the wood diameter (D_{LW}) to the local water depth (d_{cLW}) is similar to the ratio of the density of wood (ρ_{LW}) to the density of water, which implies that most LW pieces can be entrained once the

[7] The Reynolds number used for settling particles (Re_g) takes the grain diameter, D, as the characteristic length scale and the settling velocity, u_s, as the representative velocity.

local water depth reaches about half the diameter of the wood piece. The critical depth for entrainment of wood can be approximated for moderate wood densities (after Braudrick and Grant, 2001) as follows:

$$d_{cLW} = D_{LW}\frac{\rho LW}{\rho} \tag{10.26}$$

In addition to the influence of wood density and LW piece diameter, LW mobility is strongly influenced by the ratio of LW length to channel width (Bisson *et al.*, 1987; Lienkaemper and Swanson, 1987; Church, 1992; Fetherston *et al.*, 1995; Gurnell *et al.*, 2002; Hassan *et al.*, 2005; Seo and Nakamura, 2009), with the result that LW lengths (L_{LW}) that are much greater than the average bankfull channel width (W_b) cannot effectively be moved downstream. Eaton and Hassan (2013) suggest that the maximum possible travel distance, L_{travel} (based on empirical data from Mack Creek) during a single flood event is:

$$\frac{L_{travel}}{W_b} = 10\exp\left(-3.8\frac{L_{LW}}{W_b}\right) \tag{10.27}$$

This empirical result suggests that pieces for which $L_{LW}/W_b > 1$ are unlikely to move more than $0.25W_b$ during a flood, even if the water depth is sufficient to entrain them. This facilitates LW retention and associated complexity in smaller channels, while creating diverse habitat structure and hydraulics favorable for juvenile salmonids and other fishes. Hydraulic complexity created by LW in smaller streams also results in pockets of flow separation and low velocity that facilitates accumulation of organic matter that supports benthic invertebrate production at the base of aquatic food webs. In larger rivers where channel width exceeds LW length, LW may still play a role in modifying channel structure, but more typically through accumulation of LW in log jams since it is more difficult for a single piece of wood to influence structure in a large channel.

10.3.2 Sediment Transport

Our understanding of sediment transport is strongly rooted in empirical analysis of data collected during flume experiments or in the field. It is common for the datasets upon which the various empirical sediment transport laws are based to exhibit significant scatter, and it is common for independent predictions made using these equations to differ from the observed transport rates by an order of magnitude or more (e.g., Gomez and Church, 1989). Various equations have been developed for predicting the transport of **bed material** (which comprises the coarser sediment found in the channel that moves in saltation or in traction) in gravel bed rivers, all of which are based on some combination of three variables, depth, gradient, and velocity, and all of which perform about as well as each other (Church, 1985). Some of these approaches relate transport rate to stream discharge (e.g., Schoklitsch, 1934), stream power (e.g., Bagnold, 1980; Eaton and Church, 2011), or shear stress (e.g., Meyer-Peter and Muller, 1948; Einstein, 1950; Ackers and White, 1973; Parker *et al.*, 1982). The Meyer–Peter and Muller

(1948) equation is based on excess shear stress ($\tau_o - \tau_{c50}$) formulation and is still in use. A simplified version of the equation is presented here:

$$i_b = 0.253(\tau_o - \tau_{c50})^{3/2} \tag{10.28}$$

The term i_b is the transport rate per unit width of the stream channel (kg s^{-1} m^{-1}). Note that the equation is nonlinear, with transport rate increasing exponentially with excess shear stress.

While many of the transport equations listed previously (Equation 10.28 included) use information on bed surface sediment size when calculating the transport rate, they do not account for the fact that the size distribution of sediment in transport varies with flow strength. Based on observations of sediment transport made in the field, Jackson and Beschta (1982), developed a conceptual model in which they proposed that sediment transport in gravel bed streams could be categorized into two distinct phases; the first phase involves the transport of sand and fine gravel over a generally immobile bed surface; and the second occurs once the D_{50} of the surface becomes mobile, resulting in the transport of nearly all sizes of sediment found on the bed. The source area for the material transported during the first phase is thought to be low-energy environments such as pools, channel margins, and separation zones associated with in-stream obstructions where finer material can be stored, at least temporarily. In contrast, the sediment mobilized during the second phase is thought to be supplied from nearly all regions of the bed where shear stresses are sufficient to mobilize the surface D_{50}. Others have refined this concept, subdividing the second phase of sediment transport based on whether or not the D_{50} is partially mobile or fully mobile (Ashworth and Ferguson, 1989). In any case, since entrainment is size dependent, at least to some degree, it is clear that both the volume and the grain size distribution of transported sediment will vary with stream flow. In order to account for this effect, researchers have developed models for predicting the sediment transport rate for all size fractions present in the stream bed (e.g., Parker, 1990), thereby generating predictions of both the rate and the size distribution of bed material transport.

These fractional bed material transport equations do not use the excess shear stress approach illustrated by Equation 10.28, in part because it is difficult to define the threshold of entrainment objectively. Instead, the most commonly used equations relate transport rate to the ratio of the boundary shear stress and some reference shear stress, associated with a low but measurable sediment transport rate. One very commonly used equation of this form was proposed by Wilcock and Crowe (2003). This equation predicts a dimensionless sediment transport rate, W_i^*, for all grains of size D_i, as a function of Φ, where:

$$\Phi = \frac{\tau_o}{\tau_{ri}} \tag{10.29}$$

$\boldsymbol{\tau_{ri}}$ represents a reference shear stress very similar to the critical shear stress. The term τ_{ri} is calculated by combining and adapting Equations 10.21 and 10.22 as follows:

$$\tau_{ri} = \theta_r g(\rho_s - \rho) D_{50} \left(\frac{D_i}{D_{50}}\right)^b \tag{10.30}$$

In this equation, θ_r replaces θ_c, and represents a reference Shields number rather than the traditional critical Shields number. Wilcock and Crowe (2003) note that the exponent b changes with the relative grain size (D_i/D_{50}), such that b has a value close to 0.67 for particles larger than D_{50}, and a value of about 0.12 for grains less than D_{50}, as noted earlier. They provide an equation for approximating b:

$$b = \frac{0.67}{1 + \exp(1.5 - D_i/D_{50})} \tag{10.31}$$

as well as an equation for estimating θ_r as a function of the proportion of the surface that is covered by sand, F_s; the presence of sand on the bed surface facilitates the sediment entrainment process and increases the sediment transport rates for all size fractions:

$$\theta_r = 0.021 + 0.015\exp(-20F_s) \tag{10.32}$$

The dimensionless sediment transport parameter, W_i^*, is estimated using two different equations for different ranges of Φ:

$$W_i^* = 14\left(1 - \frac{0894}{\Phi}\right)^{4.5} \quad \text{for } \Phi > 1.35 \tag{10.33a}$$

$$W_i^* = 0.002\Phi^{7.5} \quad \text{for } \Phi < 1.35 \tag{10.33b}$$

The dimensionless transport rate can be translated to dimensional units as follows:

$$q_{bi} = \frac{F_i W_i^* (u^*)^3}{sg} \tag{10.34}$$

The parameter F_i represents the proportion of the surface covered by sediment of size D_i; the total transport rate per unit width of stream ($m^3\ s^{-1}\ m^{-1}$) is given by the sum of q_i over all grain sizes on the bed.

In sand-bed streams, there is a much narrower range of particles on the bed, and the issues of partial mobility, full mobility and grain size-dependent entrainment thresholds are much less important. However, sand-bed streams develop a wide array of bedforms at different flows, ranging from small ripples that scale with the thickness of the laminar sublayer to large dunes, the size of which is associated with the separation and reattachment of the boundary layer. These bedforms strongly influence near-bed hydraulics (e.g., Engleund and Hansen, 1967) and can affect both the total flow resistance and the shear stress available to transport sediment. It is also possible for the mode of sediment transport to change from traction to saltation to suspension for the same size of particle, as shear stress increases during a flood event. There are a number of different sand-bed sediment transport equations. One relatively well known set of equations was proposed by Van Rijn, who developed two complementary sets of equations for describing the transport of sand in saltation (Van Rijn, 1984a), and in suspension (Van Rijn, 1984b).

Of course, much of the sediment carried by a river does not move as bedload, even in gravel bed streams; it moves as suspended load. Unlike bedload, the rate of suspended sediment transport is rarely limited by the flow velocity of shear stress; it is typically the supply of fine sediment that limits the suspended sediment load. The supply varies from

river to river, from year to year, and even over the course of a single flood event. Normally, empirical fits are used to analyze suspended sediment loads (e.g., Walling, 1977, Crawford, 1991). They are often expressed as:

$$C = pQ^{j} \tag{10.35}$$

where C is the suspended sediment concentration (in mg L^{-1}), and p and j are event- or stream-specific parameters. While mathematical prediction of suspended sediment transport is relatively complicated, it is much easier to measure suspended sediment concentrations than it is to measure bed material load concentrations, and studies of suspended sediment dynamics in river systems are virtually all based on direct measurements (i.e., empirically fitted models) rather than model predictions.

While geomorphologists understandably focus on the transport of inorganic sediments, the dynamics of organic matter transport in streams are of comparable ecological significance. Organic matter in streams originates as aquatic plants or riparian leaves, branches, or trees that fall into streams, and are broken down by mechanical action or consumption by aquatic invertebrates (e.g., shredding stoneflies and caddisflies; Cummins, 1974; Allan and Castillo, 2007). Stream invertebrates may form "processing chains," where shredders reduce leaves to progressively finer particles that eventually end up in suspension and are consumed by downstream filter-feeders or depositional gatherers (Wallace and Webster, 1996). However, a key feature of organic matter is a much lower density than rock, so that organic matter is entrained at much lower velocities, including base flow conditions in many smaller streams. This means that there is a steady transport of smaller benthic organic matter and finer suspended particles in most streams, which increases with rising discharge well before shear stress is sufficient to mobilize larger bed material.

10.4 Ecological and Physical Interactions in Fluvial Systems

Throughout this chapter we have focused on identifying the primary geomorphic and hydraulic processes that structure the stream channel and sediment transport dynamics to provide a foundation for understanding the habitat template that constrains biological processes in streams. While subsequent chapters highlight these biological processes in greater detail, there are some additional points worth making that are directly linked to the concepts discussed in this chapter.

Bed sedimentology: In addition to the effects of sediment compaction and bed surface sand content on bed stability and entrainment thresholds, substrate properties also have profound implications for biological production. Abundant pore spaces that are not infilled by sand are essential to allow interstitial flow of water over salmonid eggs buried in gravel, and to allow newly hatched fry to emerge without being entombed (Sear *et al.*, 2008). Interstitial pore space also provides habitat for benthic invertebrates and traps the coarse and fine organic matter on which they feed, so that total benthic invertebrate abundance is often correlated with both interstitial volume and benthic organic matter abundance (Suttle and Power, 2004). Infilling of interstitial space

with fines may greatly reduce available habitat for benthic invertebrates and increase their vulnerability to visual predators.

Low flow refugia: During extreme flow events that mobilize a large proportion of the bed, hydraulic refuges that maintain low velocities and relative bed stability become very important (Lancaster and Hildrew, 1993). These include irregular channel margins that create flow separation and complex marginal structure like root wads that obstruct flow and create drag, as well as backwater habitats like abandoned side channels that remain connected to main stem habitat (Murphy *et al.*, 1986; Nickleson *et al.*, 1992). At greater than bankfull flows the floodplain itself, where shallow water and vegetation create significant resistance to flow, may become a refuge from main stem scour. Although habitat use by aquatic organisms at high flows is poorly understood because of the difficulty of studying their ecology during floods, it is well documented that survival of juvenile salmonids is higher in coastal streams with complex habitat than in structurally simple ones (Nickleson *et al.*, 1992; Solazzi *et al.*, 2000).

Channel structure: It should also be noted that biological processes can influence channel structure (Statzner, 2012); for example, beavers are noted ecosystem engineers and can significantly modify sediment transport and greatly enhance fish habitat availability through creation of dams and ponds in smaller systems (Naiman *et al.*, 1988; Pollock *et al.*, 2004). At a smaller spatial scale, aquatic plants, algal mats, and the silk nets spun by caddisfly larvae to trap food particles may significantly stabilize benthic substrates and elevate critical shear stress (Statzner *et al.*, 1999). Despite these significant feedback effects of living organisms on the abiotic stream environment (Moore, 2006), the dominant control of the habitat template in running waters remains physical, and the ecology of running waters cannot be properly understood without the context of physical and hydraulic processes.

List of Symbols

A	cross-sectional area for flow (m^2)
C	Suspended sediment concentration (g L^{-1})
C_D	coefficient of drag
D	diameter of sediment (m)
D_i	diameter of the ith percentile of the bed surface cumulative grain size distribution (m)
D_{50}	median bed surface grain diameter (m)
D_{84}	diameter for the 84th percentile of the surface grain size distribution (m)
D_{LW}	diameter of a large wood piece (m)
d	mean hydraulic depth of flow (m)
d_c	critical depth at which the Froude number is equal to 1 (m)
d_{cLW}	critical flow depth at which wood pieces may be entrained (m)
E'_{tot}	total energy per unit volume (J m^{-3})
E'_{pot}	potential energy per unit volume (J m^{-3})
E'_k	kinetic energy per unit volume (J m^{-3})
E'_ψ	Energy stored as pressure per unit volume (J m^{-3})
E_{tot}	total energy (J)

Fr	Froude number
F_s	proportion of the bed surface covered by sand
g	the acceleration of gravity (9.81 m s^{-2})
H	total head, expressing the total energy as a length scale (m)
i_b	sediment transport rate per unit width of channel (kg s^{-1} m^{-1})
k_s	characteristic roughness length (m)
L	length of a stream reach, measured in the direction of flow (m)
L_{LW}	length of a large wood piece (m)
L_{travel}	maximum possible distance of travel for a large wood piece (m yr^{-1})
P	wetted perimeter of the stream, measured perpendicular to the direction of flow (m)
Q	total stream discharge (m^3 s^{-1})
q	discharge per unit width (m^2 s^{-1})
q_{bi}	fractional sediment transport rate for grain size D_i (m^3 s^{-1} m^{-1})
R	hydraulic radius for a stream cross section (m)
Re	Reynolds number
Re^*	Reynolds particle number
S	topographic gradient of a stream bed (m m^{-1})
S_w	topographic gradient of the water surface (m m^{-1})
S_o	energy gradient of a stream (m m^{-1})
s	submerged specific gravity of sediment (typically assumed to be 1.65)
U	mean flow velocity (m s^{-1})
$u(z)$	time-averaged velocity at an elevation z above the stream bed (m s^{-1})
u_s	settling velocity for sediment particles in standing water (m s^{-1})
u^*	shear velocity (m s^{-1})
W	width of the water surface, measured perpendicular to the direction of flow (m)
W_b	bankfull width of a stream (m)
W_i^*	dimensionless transport rate for grain size D_i
z	elevation above a specified datum (m)
z_o	elevation above the bed in a turbulent boundary layer at which u(z) = 0 m s^{-1} (m)
β	topographic slope of a stream (degrees)
δ	thickness of laminar sublayer (m)
κ	Von Karman's constant (0.4)
μ	molecular viscosity (0.001 Ns m^{-2} for water)
ν	kinematic viscosity (0.000001 for water)
η	turbulent viscosity (Ns m^{-2})
ρ	density of fluid (typically 1000 kg m^{-3} for water)
ρ_s	density of sediment (typically assumed to be 2650 kg m^{-3})
ρ_{LW}	density of large wood (typically about 500 kg m^{-3})
τ_o	shear stress acting on the stream boundary (Pa)
τ_{c50}	shear stress required to entrain the D_{50} of the bed surface (Pa)

τ_{ci} shear stress required to entrain particles of size D_i from the bed surface (Pa)
τ_{ri} reference shear stress for particles of size D_i (Pa)
Γ flow resistance parameter, U/u^*
θ_c critical Shields number for particle entrainment
θ_r reference Shields number of sediment transport
Ω Total stream power of a stream (W m^{-1})
ω Stream power per unit area of a stream bed (W m^{-2})

References

Ackers, P. and White, W. R. (1973). Sediment transport: new approach and analysis. *Journal of the Hydraulics Division*, **99**(hy11), 2041–60.

Airy, G. B. (1841) Tides and waves. In *Encyclopaedia Metropolitana*, ed. H. J. Rose *et al. Mixed Sciences*, **3**, 1817–45.

Allan, J. and Castillo, M. (2007). *Stream Ecology: Structure and Function of Running Waters*, 2nd edn. Dordrecht: Springer.

Andrews, E. D. (1980). Effective and bankfull discharge of streams in the Yampa River basin, Colorado and Wyoming. *Journal of Hydrology*, **46**, 311–30.

Andrews, E. D. (1983). Entrainment of gravel from naturally sorted riverbed material. *Geological Society of America Bulletin*, **94**, 1225–31.

Armstrong, J. D. and Nislow, K. H. (2006). Critical habitat during the transition from maternal provisioning in freshwater fish, with emphasis on Atlantic salmon (*Salmo salar*) and brown trout (*Salmo trutta*). *Journal of Zoology*, **269**(4), 403–13.

Ashworth, P. J. and Ferguson, R. I. (1989). Size-selective entrainment of bed load in gravel bed streams. *Water Resources Research*, **25**(4), 627–34.

Bagnold, R. A. (1980). An empirical correlation of bedload transport rates in flumes and natural rivers. *Proceedings of the Royal Society of London*, **372** (1751), 453–73.

Benson, M. A. and Thomas, D. M. (1966). A definition of dominant discharge. *Hydrological Sciences Journal*, **11**(2), 76–80.

Bisson, P. A., Bilby, R. E., Bryant, M. D. *et al.* (1987). Large woody debris in forested streams in the Pacific Northwest: past, present, and future. In *Streamside Management: Forestry and Fishery Interactions*, ed. E. O. Salo and T. W. Cundy. Seattle, WA: College of Forest Resources, University of Washington, pp. 143–90.

Bizzi, S. and Lerner, D. N. (2013). The use of stream power as an indicator of channel sensitivity to erosion and deposition processes. *River Research and Applications*, **31**(1), 16–27.

Blanckaert, K., Garcia, X.-F., Ricardo, a.-M., Chen, Q. and Pusch, M. T. (2013). The role of turbulence in the hydraulic environment of benthic invertebrates. *Ecohydrology*, **6**(4), 700–12.

Bocchiola, D., Rulli, M. C. and Rosso, R. (2006). Transport of large woody debris in the presence of obstacles. *Geomorphology*, **76**(1), 166–78.

Braudrick, C. A. and Grant, G. E. (2001). Transport and deposition of large woody debris in streams: a flume experiment. *Geomorphology*, **41**(4), 263–83.

Brumner, G. W. (2010). *HEC-RAS River Analysis System. Hydraulic Reference Manual. Version 4.1.* Davis, CA: Hydrologic Engineering Center.

Carling, P. A. (1983). Threshold of coarse sediment transport in broad and narrow natural streams. *Earth Surface Processes and Landforms*, **8**, 1–18.

Church, M. (1985). Bed load in gravel-bed rivers: observed phenomena and implications for computation. *Proceedings, Canadian Society for Civil Engineering Annual Meeting, Saskatoon, Saskatchewan*, **2**, 17–37.

Church, M. (1992). Channel morphology and typology. In *The Rivers Handbook 1*. Oxford, Blackwell Science, pp. 126–143.

Crawford, C. G. (1991). Estimation of suspended-sediment rating curves and mean suspended-sediment loads. *Journal of Hydrology*, **129**(1), 331–48.

Cummins, K. W. (1974). Structure and function of stream ecosystems. *BioScience*, **24**(11), 631–41.

Eaton, B. C. and Church, M. (2011). A rational sediment transport scaling relation based on dimensionless stream power. *Earth Surface Processes and Landforms*, **36**(7), 901–10.

Eaton, B. C. and Hassan, M. A. (2013). Scale-dependent interactions between wood and channel dynamics: modeling jam formation and sediment storage in gravel-bed streams. *Journal of Geophysical Research: Earth Surface*, **118**(4), 2500–8.

Einstein, H. A. (1950). *The Bedload Function for Sediment Transportation in Open Channels. Technical Bulletin No. 1026.* Washington, DC: United States Department of Agriculture, Soil Conservation Service.

Enders, E. C., Boisclair, D. and Roy, A. G. (2003). The effect of turbulence on the cost of swimming for juvenile Atlantic salmon (*Salmo salar*). *Canadian Journal of Fisheries and Aquatic Sciences*, **60**(9), 1149–60.

Engelund, F. and Hansen, E. (1967). *A Monograph on Sediment Transport in Alluvial Streams*. Copenhagen: Teknisk forlag.

Ferguson, R. I. (2007). Flow resistance equations for gravel- and boulder-bed streams. *Water Resources Research*, **43**, doi:10.1029/2006WR005422.

Ferguson, R. I. and Church, M. (2004). A simple universal equation for grain settling velocity. *Journal of Sedimentary Research*, **74**(6), 933–7.

Fetherston, K. L., Naiman, R. J. and Bilby, R. E. (1995). Large woody debris, physical process, and riparian forest development in montane river networks of the Pacific Northwest. *Geomorphology*, **13**, 133–44.

Gibbins, C., Vericat, D. and Batalla, R. J. (2007). When is stream invertebrate drift catastrophic? The role of hydraulics and sediment transport in initiating drift during flood events. *Freshwater Biology*, **52**(12), 2369–84.

Gomez, B. and Church, M. (1989). An assessment of bed load sediment transport formulae for gravel bed rivers. *Water Resources Research*, **25**(6), 1161–86.

Gurnell, A. M., Piegay, H., Swanson, F. J. and Gregory, S. V. (2002). Large wood and fluvial processes. *Freshwater Biology*, **47**(4), 601–19.

Haschenburger, J. K. and Wilcock, P. R. (2003). Partial transport in a natural gravel bed channel. *Water Resources Research*, **39** (1), doi:10.1029/2002WR001532.

Hassan, M. A., Hogan, D. L., Bird, S. A. *et al.* (2005). Spatial and temporal dynamics of wood in headwater streams of the Pacific Northwest. *Journal of American Water Resources Association*, **41**(4), 899–919.

Hauer, C., Unfer, G., Graf, W. *et al.* (2011). Hydro-morphologically related variance in benthic drift and its importance for numerical habitat modelling. *Hydrobiologia*, **683**(1), 83–108.

Hayes, J. and Jowett, I. (1994). Microhabitat models of large drift-feeding brown trout in three New Zealand Rivers. *North American Journal of Fisheries Management*, **14**, 710–25.

Henderson, F. M. (1966). *Open Channel Flow*. New York: MacMillan Publishing Co.

Hickin, E. J. (1984). Vegetation and river channel dynamics. *The Canadian Geographer/Le Géographe canadien*, **28**(2), 111–26.

Hinch, S. and Rand, P. (2000). Optimal swimming speeds and forward-assisted propulsion: energy-conserving behaviors of upriver-migrating adult salmon. *Canadian Journal of Fisheries and Aquatic Sciences*, **57**, 2470–8.

Hutchinson, G. E. (1965). *The Ecological Theatre and the Evolutionary Play*. New Haven, CT: Yale University Press.

Hynes, H. (1970). *The ecology of running waters*. Liverpool: Liverpool University Press.

Jackson, W. L. and Beschta, R. L. (1982). A model of two-phase bedload transport in an Oregon coast range stream. *Earth Surface Processes and Landforms*, **7**(6), 517–27.

Kohler, S. (1985). Identification of stream drift mechanisms: an experimental and observational approach. *Ecology*, **66**(6), 1749–61.

Komar, P. D. (1987). Selective grain entrainment by a current from a bed of mixed sizes: a reanalysis. *Journal of Sedimentary Petrology*, **57**(2), 203–11.

Lancaster, J. and Hildrew, A. (1993). Characterizing in-stream flow refugia. *Canadian Journal of Fisheries and Aquatic Sciences*, **50**, 1663–75.

Lane, E. W. (1957). *A Study of the Shape of Channels Formed by Natural Streams Flowing in Erodible Material*. Omaha, NB: US Army Engineer Division, Missouri River.

Leopold, L. B. and Maddock, T. (1953). *The Hydraulic Geometry of Stream Channels and Some Physiographic Implications*. U.S. Geological Survey Professional Paper, No. 252. Washington, DC: US Government Printing Office.

Leopold, L. B. and Wolman, M. G. (1957). *River Channel Patterns: Braided, Meandering, and Straight*. US Geological Survey Professional Paper, No. 282-b. Washington, DC: US Government Printing Office.

Liao, J. C., Beal, D., Lauder, G. V. and Triantafyllou, M. (2003a). The Karman gait: novel body kinematics of rainbow trout swimming in a vortex street. *Journal of Experimental Biology*, **206**, 1059–73.

Liao, J. C., Beal, D. N., Lauder, G. V. and Triantafyllou, M. (2003b). Fish exploiting vortices decrease muscle activity. *Science*, **302**, 1566–9.

Lienkaemper, G. W. and Swanson, F. J. (1987). Dynamics of large woody debris in streams in old-growth Douglas-fir forests. *Canadian Journal of Forest Research*, **17**, 150–6.

Luce, J. J., Lapointe, M. F., Roy, A. G. and Ketterling, D. B. (2013). The effects of sand abrasion of a predominantly stable stream bed on periphyton biomass losses. *Ecohydrology*, **6**, 689–99.

Mackin, J. H. (1948). Concept of the graded river. *Geological Society of America Bulletin*, **59**, 463–512.

Magilligan, F. J. (1992). Thresholds and the spatial variability of flood power during extreme floods. *Geomorphology*, **5**, 373–90.

McIntosh, A. R. and Townsend, C. R. (1998). Do different predators affect distance, direction, and destination of movements by a stream mayfly? *Canadian Journal of Fisheries and Aquatic Sciences*, **55**(8), 1954–60.

McLean, D. G., Church, M. and Tassone, B. (1999). Sediment transport along lower Fraser River. *Water Resources Research*, **35** (8), 2533–48.

Meffe, G. (1984). Effects of abiotic disturbance on coexistence of predator-prey fish species. *Ecology*, **65** (5), 1525–34.

Meyer-Peter, R. and Müller, R. (1948). Formulas for bedload transport. Proceedings 2nd Meeting International Association of Hydraulic Research, Stockholm, 39–64.

Moore, J. W. (2006). Animal ecosystem engineers in streams. *BioScience*, **56**(3), 237–46.

Moore, K. M. and Gregory, S. V. (1988). Summer habitat utilization and ecology of cutthroat trout fry (*Salmo clarki*) in Cascade Mountain streams. *Canadian Journal of Fisheries and Aquatic Sciences*, **45**(11), 1921–30.

Murphy, M., Heifetz, J., Johnson, F. W., Koski, K. and Thedinga, J. F. (1986). Effects of clear-cut logging with and without buffer strips on juvenile salmonids in Alaskan streams. *Canadian journal of Fisheries and Aquatic Sciences*, **43**, 1521–33.

Naiman, R., Johnston, C. and Kelley, J. (1988). Alteration of North American streams by beaver. *BioScience*, **38**, 753–62.

Nanson, G. C. and Knighton, A. D. (1996). Anabranching rivers: their cause, character and classification. *Earth Surface Processes and Landforms*, **21**, 217–39.

Nanson, G. C. and Croke, J. C. (1992). A genetic classification of floodplains. *Geomorphology*, **4**, 459–86.

Nickelson, T. T., Rodgers, J. D., Johnson, S. L. and Solazzi, M. F. (1992). Seasonal changes in habitat use by juvenile coho salmon (*Oncorhynchus kisutch*) in Oregon coastal streams. *Canadian Journal of Fisheries and Aquatic Sciences*, **49**, 783–9.

Parker, G. (1991). Selective sorting and abrasion of river gravel. II: Applications. *Journal of Hydraulic Engineering*, **117**(2), 150–71.

Parker, G. (1990). Surface-based bedload transport relation for gravel rivers. *Journal of Hydraulic Research*, **28**(4), 417–36.

Parker, G., Klingeman, P. C. and McLean, D. G. (1982). Bedload and size distribution in paved gravel-bed streams, *J. Hydraul. Div. Am. Soc. Civ. Eng.*, **108**(HY4), 544–71.

Parker, G. and Klingeman, P. C. (1982). On why gravel bed rivers are paved. *Water Resources Research*, **18**(5), 1409–23.

Peakall, J., Ashworth, P. and Best, J. (1996). Physical modelling in fluvial geomorphology: principles, applications and unresolved issues. In *The Scientific Nature of Geomorphology*, ed. B. L. Rhoads and C. Thorn. Chichester, UK: Wiley, pp. 221–253.

Pickup, G. and Warner, R. F. (1976). Effects of hydrologic regime on magnitude and frequency of dominant discharge. *Journal of Hydrology*, **29**, 51–75.

Pollock, M., Pess, G., Beechie, T. and Montgomery, D. (2004). The importance of beaver ponds to coho salmon production in the Stillaguamish River basin, Washington, USA. *North American Journal of Fisheries Management*, **24**, 749–60.

Pujolar, J. M., Vincenzi, S., Zane, L. *et al.* (2011). The effect of recurrent floods on genetic composition of marble trout populations. *PloS One*, **6**(9), e23822.

Roghair, C., Dolloff, C. and Underwood, M. (2002). Response of a brook trout population and instream habitat to a catastrophic flood and debris flow. *Transactions of the American Fisheries Society*, **131**, 718–30.

Rosenfeld, J. S., Bouwes, N., Wall, C. E. and Naman, S. M. (2014). Successes, failures, and opportunities in the practical application of drift-foraging models. *Environmental Biology of Fishes*, **97**, 551–74.

Schoklitsch, A. (1934). Der geschiebetrieb und die geschiebefracht. *Wasserkraft Wasserwirtschaft*, **4**, 1–7.

Sear, D. A., Frostick, L. B., Rollinson, G. and Lisle, T. E. (2008). The significance and mechanics of fine-sediment infiltration and accumulation in gravel spawning beds. In *Salmonid Spawning Habitat in Rivers: Physical Controls, Biological Responses, and Approaches to Remediation*, ed. D. A. Sear and P. CeVries. Bethesda, MD: American Fisheries Society, pp 149–73.

Seo, J. I. and Nakamura, F. (2009). Scale-dependent controls upon the fluvial export of large wood from river catchments. *Earth Surface Processes and Landforms*, **34**(6), 786–800.

Simons, D. B. and Richardson, E. V. (1963). Forms of bed roughness in alluvial channels. *Transactions of the American Society of Civil Engineers*, **128**(1), 284–302.

Solazzi, M. F., Nickelson, T. E., Johnson, S. L. and Rodgers, J. D. (2000). Effects of increasing winter rearing habitat on abundance of salmonids in two coastal Oregon streams. *Canadian Journal of Fisheries and Aquatic Sciences*, **57**, 906–14.

Statzner, B., Arens, M., Champagne, J.-Y., Morel, R. and Herouin, E. (1999). Silk-producing stream insects and gravel erosion: significant biological effects on critical shear stress. *Water Resources Research*, **35**, 3495–506.

Statzner, B. (2012). Geomorphological implications of engineering bed sediments by lotic animals. *Geomorphology*, **157**–158, 49–65.

Suttle, K., Power, M., Levine, J. and McNeeley, C. (2004). How fine sediment in riverbeds impairs growth and survival of juvenile salmonids. *Ecological Applications*, **14**(4), 969–74.

Taguchi, M. and Liao, J. C. (2011). Rainbow trout consume less oxygen in turbulence: the energetics of swimming behaviors at different speeds. *Journal of Experimental Biology*, **214**, 1428–36.

Van den Berg, J. H. (1995). Prediction of alluvial channel pattern of perennial rivers. *Geomorphology*, **12**, 259–79.

Van Rijn, L. C. (1984a). Sediment transport, part I: bed load transport. *Journal of Hydraulic Engineering*, **110**(10), 1431–56.

Van Rijn, L. C. (1984b). Sediment transport, part II: suspended load transport. *Journal of Hydraulic Engineering*, **110**(11), 1613–41.

Wallace, J. B. and Webster, J. R. (1996). The role of macroinvertebrates in stream ecosystem function. *Annual Review of Entomology*, **41**(131), 115–39.

Walling, D. E. (1977). Assessing the accuracy of suspended sediment rating curves for a small basin. *Water Resources Research*, **13**(3), 531–8.

Whipple, K. X. and Tucker, G. E. (1999). Dynamics of the stream-power river incision model: implications for height limits of mountain ranges, landscape response timescales, and research needs. *Journal of Geophysical Research: Solid Earth*, **104**, 17661–74.

Wilcock, P. R. and McArdell, B. W. (1993). Surface-based fractional transport rates: mobilization thresholds and partial transport of a sand-gravel sediment. *Water Resources Research*, **29**(4), 1297–1312.

Wilcock, P. R. and Crowe, J. C. (2003). Surface-based transport model for mixed-size sediment. *Journal of Hydraulic Engineering*, **129**(2), 120–8.

Wolman, M. G. and Miller, J. P. (1960). Magnitude and frequency of forces in geomorphic processes. *Journal of Geology*, **69**, 54–74.